Spatial distribution and dynamics of space charges in poly(2, 5-pyridinediyl)

2002 J. Phys.: Condens. Matter 14 8455

(http://iopscience.iop.org/0953-8984/14/36/305)

INSTITUTE OF PHYSICS PUBLISHING JOURNAL OF PHYSICS: CONDENSED MATTER

J. Phys.: Condens. Matter **14** (2002) 8455–8462 PII: S0953-8984(02)37408-3

Spatial distribution and dynamics of space charges in poly(2, 5-pyridinediyl)

F Feller[1,3], **D Geschke**[1] **and A P Monkman**[2]

[1] Institut für Experimentelle Physik I, Fakultät für Physik und Geowissenschaften, Universität Leipzig, Linnéstrasse 5, D-04103 Leipzig, Germany
[2] Organic Electroactive Materials Research Group, Department of Physics, University of Durham, South Road, Durham DH1 3LE, UK

E-mail: feller@uni-leipzig.de

Received 24 May 2002, in final form 19 July 2002
Published 29 August 2002
Online at stacks.iop.org/JPhysCM/14/8455

Abstract

We present investigations of the spatial distribution of space charges in thin films of conjugated polymers. A thermal wave method, the laser intensity modulation method, has been used to resolve the depth profile of space charges and the distribution of the internal electric field in 3–4 μm films of poly(2, 5-pyridinediyl). The dynamics of the space-charge accumulation has been investigated by means of measurements of the temporal evolution and the temperature dependence of the pyroelectric response. The results demonstrate that in conjugated polymers, space charges of either sign can be stored permanently by deep trapping. This charge significantly reduces the internal electric field in the bulk of the films.

1. Introduction

The performance of electroluminescent devices made from conjugated polymers is strongly related to the efficiency of charge injection and transport in the organic material. Effective charge injection from the electrodes into the polymer is achieved by choosing electrode materials which have a work function that closely matches the conduction or valence band levels of the polymer. In such a configuration the resulting barrier height for injection of charge carriers into the polymer is low, giving rise to a high injection current [1]. If the barrier height is lower than about 0.3 eV, in most conjugated polymers the injection rate becomes higher than the transport rate in the bulk of the polymer; thus charge is injected faster than it can be transported in the low-mobility material [2]. The result is an accumulation of space charge in the polymer next to the injecting contact, which shields the external electric field, limiting both charge transport and further charge injection. Space charge is therefore considered to have a

[3] Author to whom any correspondence should be addressed.

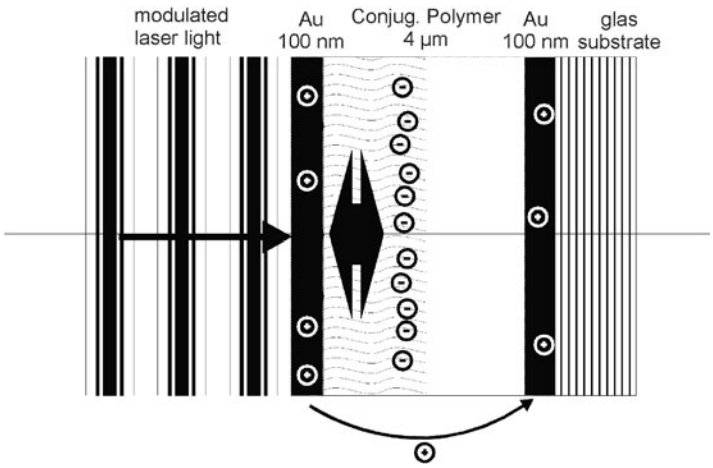

Figure 1. An illustration of the pyroelectric response of a negative-space-charge layer. The small shift of the layer occurring because of the inhomogeneous thermal expansion of the material leads to the induction of countercharges on the electrodes which are measured as a small ac signal.

negative influence on the performance of PLEDs and it should be of interest to measure the extent and dynamics of this phenomenon.

Space-charge-limited conduction (SCLC) is well described for inorganic semiconductors with ohmic contacts [3, 4] and SCLC theory has been successfully applied to low-barrier organic devices too. These approaches involve current–voltage measurements [5], deep-level transient spectroscopy (DLTS) [6], impedance and transient capacitance measurements [7] and have provided valuable information about trap concentrations, about the energy and energy distribution of traps as well as about the mechanisms of charge transport through polymer layers. In this work we report results of space-charge measurements on thick films of conjugated polymers using the laser intensity modulation method (LIMM) [8]. The method allows us to investigate the spatial distribution of space charges in the direction perpendicular to the film. Furthermore, the creation and annihilation of the space charge can be observed by measuring the temporal evolution of a pyroelectric current.

2. Experimental section

The chemical structure of poly(2, 5-pyridinediyl) is depicted in the inset of figure 2. PPY was synthesized as described previously [9] and dissolved in formic acid using a concentration of 30 mg ml^{-1}. Samples for LIMM measurements are fabricated with the structure of conventional organic light-emitting diodes but with greater thickness. Films of 3–4 μm were prepared by spin- or drop-casting from solution onto gold-covered glass substrates and subsequent evaporation of a second gold electrode (front electrode). The front electrode was covered by an additional 20 nm bismuth layer to enhance absorption of the laser light. The set-up consists of a HeNe laser, its beam being intensity modulated by an acousto-optical modulator with a frequency f supplied by a frequency generator. The sample itself is mounted onto a heat sink and fixed with silver paint to ensure good thermal contact between the substrate and the metal of the sink. The pyroelectric response of the sample is detected as a small alternating current between the gold electrodes. This pyroelectric current is amplified by a current-to-voltage converter (CVC) using a gain of 10^5 V A^{-1} and measured by a lock-in

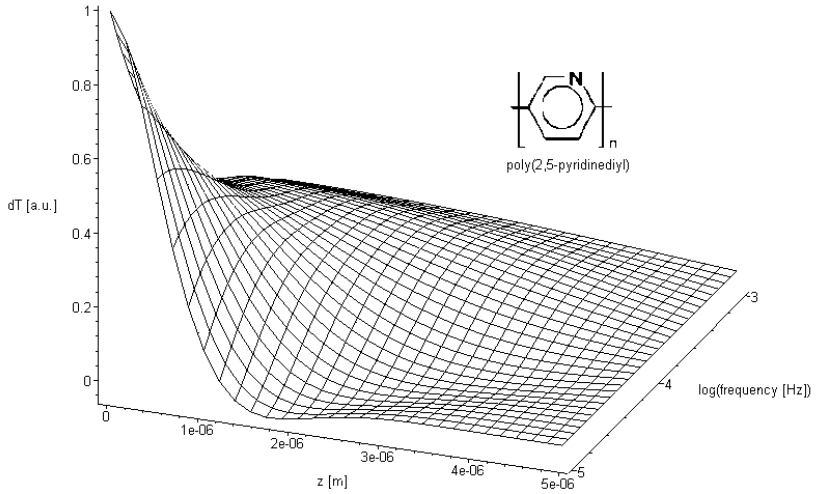

Figure 2. The real part of the complex temperature profile established in the polymer for different laser modulation frequencies. At high frequencies only the region near the front electrode ($z = 0$) is heated; at lower frequencies the heat wave penetrates deeper into the film but with lower intensity, which reduces the resolution of the method with increasing z. The inset shows the chemical structure of PPY.

amplifier with the reference frequency matched to the frequency generator that provides the modulation frequency f for the acousto-optical modulator. In addition, a galvanic decoupler has been used to allow the application of a DC bias during the very sensitive AC measurements across the same electrodes. The sweep of the frequency generator and the data recording are controlled by a computer.

In order to increase the resolution of the method in films of only a few micrometres, the electronic components have been refined in the frequency region beyond 100 kHz. A specially designed CVC is used in combination with a EG&G 5302 lock-in amplifier allowing measurements up to 600 kHz, which corresponds to a minimal measurement depth of 200 nm.

3. LIMM equations

Since the development of the LIMM by Lang and Das-Gupta [10] it has been used successfully to study the depth profile of the polarization distribution in thin ferroelectric layers [11] as well as space charges in electret films [12, 13]. Depending on the material under study, the method uses the pyroelectric property of polar materials—the change in spontaneous polarization with temperature—or the spatially inhomogeneous distribution of space charges. In the following, some basic physical aspects of the method are explained.

Figure 1 illustrates the interaction between the incident light and the polymer film. When the modulated laser beam hits the front electrode of the sample it is absorbed and transformed into a heat wave that penetrates into the sample. The front electrode is opaque; therefore no light is transmitted to the polymer itself. For a certain modulation frequency f of the incident laser beam, the complex amplitude of the pyroelectric current $I_P(f)$ in a film of thickness L and illuminated area A is well described by the fundamental LIMM equation [10]:

$$I_p(f) = 2\pi \mathrm{i} f \frac{A}{L} \int_0^L r(z) T(f, z)\, \mathrm{d}z. \tag{1}$$

Therein, $T(f, z)$ is the temperature profile generated by the heat wave, which is a complex. Figure 2 shows the real part of $T(f, z)$. For a certain frequency the real part can be approximated as a continuously falling function with a maximum at $z = 0$ (at the front electrode) that vanishes at the *heat wave penetration depth*

$$\sigma_f = \sqrt{\chi/\pi f} \tag{2}$$

with χ the thermal diffusivity of the polymer (typical value for polymers [14]: $\chi = 1 \times 10^7$ m^2 s^{-1}).

In addition, in equation (1), $r(z)$ is the desired distribution function, which in non-polar materials has only contributions from space charges $\rho(z)$ and the externally applied electric field $E_{ext}(z)$:

$$r(z) = (\alpha_x - \alpha_\varepsilon)\varepsilon_0\varepsilon(E_\rho(z) + E_{ext}(z)),$$

with $E_\rho(z)$ the field induced by the space charges according to $\varepsilon_0\varepsilon\, \mathrm{d}E_\rho(z)/\mathrm{d}z = \rho$ and α_χ and α_ε the thermal coefficients of expansion and dielectric permittivity, respectively. In the LIMM experiment the pyroelectric current $I_P(f)$ is measured as a function of the modulation frequency f. Afterwards the distribution function $r(z)$ has to be inferred via inversion of the integral equation (1) using the temperature profile $T(f, z)$ that can be calculated for specific thermal parameters. The inversion of equation (1) is, however, known to be an ill-posed inverse problem, since the distribution function $r(z)$ does not depend continuously upon the LIMM data [15]. Accordingly, small aberrations in the data, which are inevitably affected by measurement errors, will result in large or even unbounded errors of the reconstructed distribution function $r(z)$. In order to solve such ill-posed inverse problems, special mathematical methods, i.e. regularization methods, are necessary [16, 17].

4. Results and discussion

PPY samples have been poled by application of a DC bias of 25 MV m^{-1} for about 30 min at room temperature. Afterwards LIMM spectra have been recorded with the bias still applied. Figure 3 shows the results for illumination through the front electrode and the back electrode. For both directions of the incident laser light the real part of the pyroelectric current has a maximum at about 100 kHz and turns to negative values at very high frequencies. The frequency of the maximum pyroelectric current, via equation (2), corresponds to a heat wave penetration depth of about 500 nm. Thus, the measured LIMM spectra originate from space charges relatively near to the electrodes in which the laser light was absorbed. Note that PPY polymer chains do not have a permanent dipole; therefore the pyroelectricity cannot be explained by a temperature-dependent spontaneous polarization but must be solely due to space charge. Figure 3 demonstrates that the pyroelectric signal is reduced by a factor of about 15 when the laser hits the sample through the back electrode. This difference cannot be explained by the lack of a bismuth absorption layer, which can enhance the signal by a factor of 3 only. It is therefore presumed that the amount of space charge accumulated near the top electrode is higher than that near the back electrode. We will give an interpretation of this finding later on in this work.

Figure 4 shows the results of the deconvolution using the regularization program 'Ftikreg'. In the upper panel the electric field distribution is depicted, while the lower panel shows the charge profile. It can be seen that space charge is accumulated near the front electrode with the same sign as the electrode itself (homo-charges). After this charge layer, deeper inside the polymer film a second space-charge layer is observed with opposite sign (hetero-charges). This feature is less pronounced and broader and is also observed in the spectrum obtained with illumination through the back electrode.

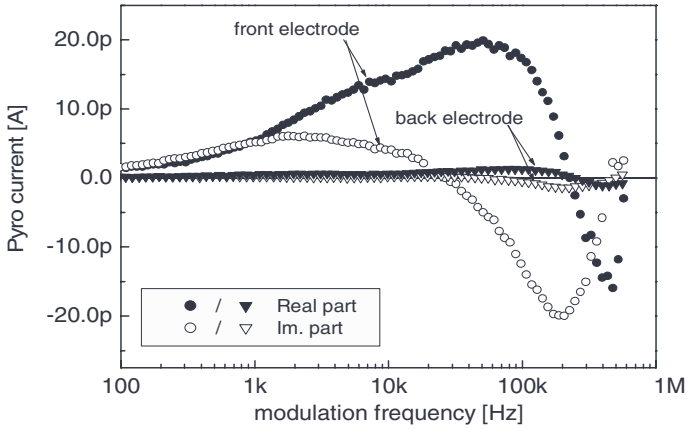

Figure 3. LIMM spectra of a Au/PPY/Au sample with a laser incident on the front electrode (circles) and on the back (glass-covered) electrode (triangles). The spectra are represented by their real (filled symbols) and imaginary parts (open symbols). Measurements were performed at room temperature using an applied electric field of 25 MV m^{-1}.

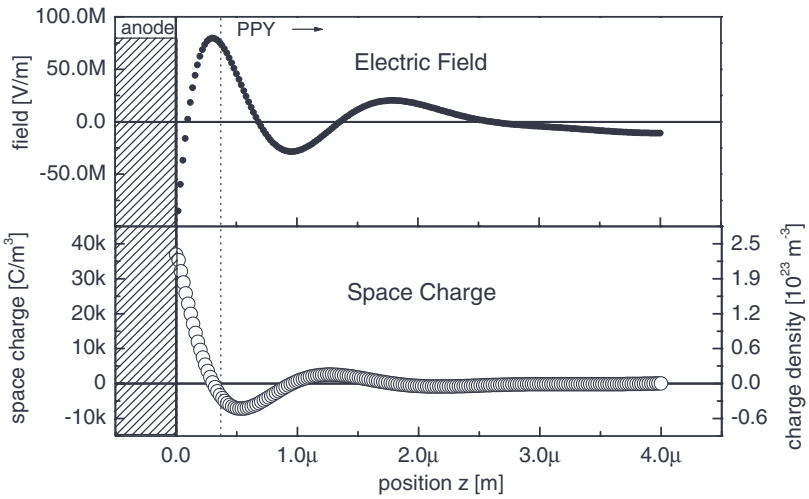

Figure 4. Distributions of electric field (upper panel) and space charge (lower panel) obtained from the front-electrode LIMM spectrum in figure 3 via regularization.

For the interpretation of the charge profile we propose a model, which is illustrated in figure 5. The work function of the gold electrodes is about midway between the HOMO level and the LUMO level of PPY. The barrier height for injection of electrons or holes is in the region of 1 eV; thus almost no injection of carriers into the transport levels is expected. Such a strongly injection-limited device should contain only very few space charges, because any injected charge is immediately led away in the external field. However, our results show significant space-charge injection into the polymer. We explain these findings by the presence of traps, with high concentration near the surface of the polymer film. Such traps are chemical defects of the polymer chain and can be introduced during the synthesis or during the device preparation. Shallow traps are present in every polymer and charge is transported by field-induced hopping between those traps. In deeper traps with an energy level up to 1 eV,

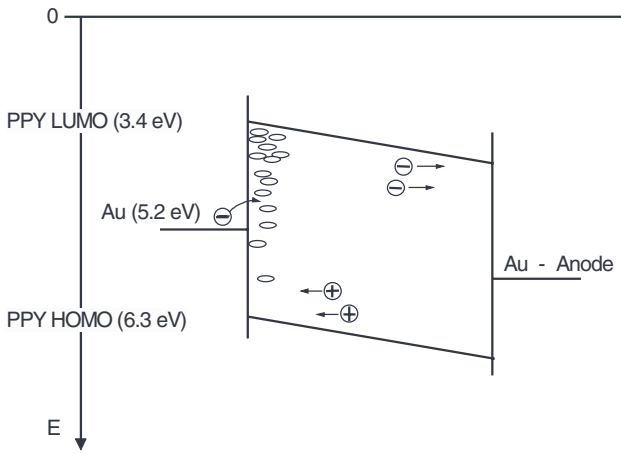

Figure 5. The model proposed to explain the pyroelectric results for PPY. Charge carriers are injected into deep traps at the surface of the polymer layer. Simultaneously, mobile charged states in the bulk are separated by the influence of the external electric field.

which are also reported for conjugated polymers, charge can be more permanently stored as demonstrated for instance using transient capacitance measurements. We assume a relatively high concentration of such deep traps near the front electrode, providing acceptor states for injected charge carriers. Thus electrons (or holes) are not injected into the conduction band but directly into trap levels close to the surface of the polymer film, where they accumulate because of the low release rate of the traps.

Considering the lower hetero-charge layer, we suggest them to be due to a separation of charge driven by the external electric field. Such charge may originate from defects in the polymer. Extrinsic defects are, for example, impurity atoms/molecules inserted during the synthesis of the polymer or during device fabrication, solvent residuals or oxygen from the ambient air. They can lead to an accidental doping of the polymer, i.e. to supply of charge carriers. On the other hand, imperfections of the chemical structure of the polymer, bending or torsion of chains may induce a break of the conjugation with a charged defect at this location. Such an intrinsic defect can be mobile because it can be transformed between adjacent chains as polarons. In a second step the two species, the charge carriers from accidental doping and the polarons, could be separated in the applied field migrating towards the surface zones of the film. Approaching the contact they can be trapped, recombine with opposite charge carriers or be injected into the electrode. The trapped part of the charge could then account for the observed feature.

We have investigated the bias dependence of the pyroelectric signal. In this experiment the modulation frequency of the laser beam was set to a constant value of 33 kHz, i.e. near the maximum of the real part of the LIMM spectrum. The result is depicted in figure 6. At room temperature we find a clear hysteresis behaviour, which means that the pyroelectric signal does not vanish upon removing the bias, but maintains a remnant value of the same sign as the last applied bias value. In the framework of our model this is the expected behaviour for deeply trapped charge. This means that the material can be poled by application of a bias and is able to store the charge after removing the bias. A significant amount of charge is preserved over a very long time (ten days without measurable decrease).

When the sample is cooled down, the response to the applied electric field is reduced rapidly. As demonstrated in figure 6, at about 190 K the pyroelectric signal shows only a small bias dependence. In particular, it is not possible to deposit new charge in the polymer

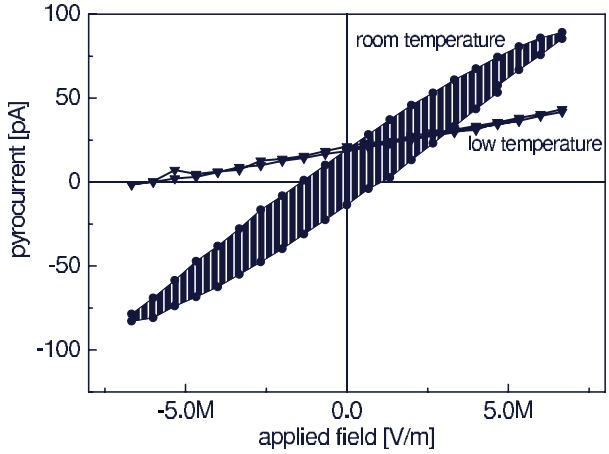

Figure 6. Bias dependences of the pyroelectric current at room temperature (circles) and at 180 K (triangles). Both measurements have been carried out under vacuum. The low-temperature curve was recorded after poling the sample at room temperature. The modulation frequency was 33 kHz.

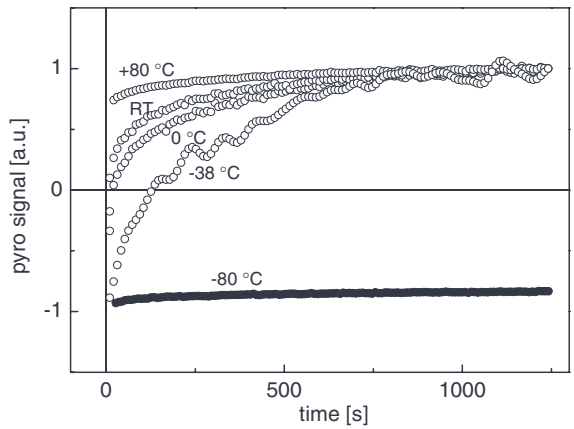

Figure 7. The dynamics of the pyroelectric response in a Au/PPY/Au device after switching the external bias polarity. At temperatures higher than 350 K, the response times are lower than 1 s, which is the limit of the temporal resolution of the experiment.

or to remove it by applying an external bias. It has also been observed that the charge profile accumulated in the polymer film under bias at room temperature is frozen in when the sample is cooled down. Both processes, injection of charge and charge transport in the bulk, must therefore be strongly temperature dependent, which is in agreement with common charge transport models for organic thin-film devices.

Figure 7 shows the temporal evolution of the pyroelectric signal after switching the polarity of the external bias. At room temperature it takes several minutes for the sample to invert its polarity. When the temperature is decreased, the switching time is increased and at 190 K no switching is possible as described previously. On the other hand, raising the temperature above room temperature significantly increases the speed of the poling process. Addressing the trapped charges in the polymer with an external bias is therefore more effective at higher temperatures.

The operation of devices made from conjugated polymer films should be influenced by space charges that accumulate in the polymer. The observed charge accumulation in PPY films using blocking electrodes indicates that space charge due to trapped carriers has significant impact on the internal electric field and therefore on the charge transport in the polymer.

5. Conclusions

We have demonstrated how the thermal wave technique LIMM can be applied for the investigation of conjugated polymer films. It allows measurement of the space-charge profile within layers of several hundred nanometres and of the spatial distribution of the internal electric field. Our results show that despite using an electrode configuration with very high carrier injection barriers, space charge is brought into the material and deeply trapped near the front surface of the film. The amount of the space charge accumulated after several minutes is large enough to distort the internal electric field, which should have an influence on the charge transport in polymer devices. Using temperature-dependent measurements of the pyroelectric signal after switching the external bias polarity, the dynamics of the poling process can be observed and it shows that the charge accumulation is strongly accelerated at high temperatures. On the other hand, at low temperatures (190 K) any established space-charge profile is frozen in and it seems that it is possible neither to inject more charge and trap it permanently in the material nor to remove charges that have been stored under higher temperatures. This effect, which makes the electronic behaviour of the polymer device strongly dependent on its bias and temperature history, should also kept in mind when performing any low-temperature measurements on thin-film conjugated polymer devices.

References

[1] Davids P S, Kogan Sh M, Parker I D and Smith D L 1996 *Appl. Phys. Lett.* **69** 2270
[2] Blom P W M and Vissenberg M C J M 2000 *Mater. Sci. Eng.* **27** 53
[3] Lampert M A 1956 *Phys. Rev.* **103** 1648
[4] Rose A 1955 *Phys. Rev.* **97** 1538
[5] Campbell A J, Bradley D D C and Lidzey D G 1997 *J. Appl. Phys.* **82** 6326
[6] Campbell A J, Bradley D D C, Werner E and Brütting W 2000 *Synth. Met.* **111–112** 273
[7] Scherbel J, Nguyen P H, Paasch G, Brütting W and Schwoerer M 1998 *J. Appl. Phys.* **83** 5045
[8] Feller F, Geschke D and Monkman A P 2001 *Appl. Phys. Lett.* **79** 779
[9] Dailey S, Halim M, Rebourt E, Horsburgh L E, Samuel I D W and Monkman A P 1998 *J. Phys.: Condens. Matter* **10** 5171–8
[10] Lang S B and Das-Gupta D K 1986 *J. Appl. Phys.* **59** 2151
[11] Lang S B 1991 *Ferroelectrics* **118** 343
[12] Bloß P, Steffen M, Schäfer H, Yang G-M and Sessler G M 1997 *J. Phys. D: Appl. Phys.* **30** 1668
[13] Oliveira O N Jr and Leal Ferreira G F 1987 *Appl. Phys.* A **42** 213
[14] Wong P K, Fung P C W and Tam H L 1998 *J. Appl. Phys.* **84** 6623
[15] Morozov V A 1977 *Methods for Solving Incorrectly Posed Problems* (Stuttgart: Teubner)
[16] Groetsch C W 1984 *The Theory of Tikhonov Regularization for Fredholm Equations of the First Kind* (London: Pitman)
[17] Honerkamp J and Weese J 1990 *Continuum Mech. Thermodyn.* **2** 17